European Journal of Medicinal Chemistry 208 (2020) 112772

Contents lists available at ScienceDirect

European Journal of Medicinal Chemistry

journal homepage: http://www.elsevier.com/locate/ejmech

Synthesis and evaluation of thiophene based small molecules as potent inhibitors of *Mycobacterium tuberculosis*

Chhuttan L. Meena [1], Padam Singh [1], Ravi P. Shaliwal, Varun Kumar, Arun Kumar, Anoop Kumar Tiwari, Shailendra Asthana, Ramandeep Singh**, Dinesh Mahajan*

Translational Health Science and Technology Institute (THSTI), NCR Biotech Science Cluster, 3rd Milestone, Faridabad-Gurugram Expressway, Faridabad, 121001, India

ARTICLE INFO

Article history:
Received 27 March 2020
Received in revised form
18 June 2020
Accepted 17 August 2020
Available online 23 August 2020

Keywords:
Tuberculosis
Thiophene
Pks13
KatG
Synergy

ABSTRACT

Herein, we report the synthesis and anti-tubercular studies of novel molecules based on thiophene scaffold. We identified two novel small molecules **4a** and **4b**, which demonstrated 2-fold higher *in vitro* activity (MIC_{99}: 0.195 μM) compared to first line TB drug, isoniazid (0.39 μM). The identified leads demonstrated additive effect with front line TB drugs (isoniazid, rifampicin and levofloxacin) and synergistic effect with a recently FDA-approved drug, bedaquiline. Mechanistic studies (i) negated the role of Pks13 and (ii) suggested the involvement of KatG in the anti-tubercular activity of these identified leads.

1. Introduction

Tuberculosis (TB) has decimated and impacted countless human lives for tens of thousands of years and is ranked among the top 10 causes of the deaths worldwide in modern era [1]. According to World Health Organization (WHO) reports, nearly 1.2 million and 0.25 million deaths occurred due to TB infection and HIV-TB co-infection, respectively in 2018 [1]. The current efforts to control TB are focused on the development of potent chemotherapeutics, sensitive diagnostics and efficacious vaccines. There is an urgent need to develop next-generation chemotherapeutics that possess a novel mechanism of action and are compatible with the current regimens. The new chemical entities should have low toxicological profile and also be effective against drug-resistant *M. tuberculosis*. Isoniazid (INH), pyrazinamide (PZA), rifampicin (RIF) and ethambutol (EMB) are the four first line TB drugs which were identified in 1951, 1952, 1957 and 1962, respectively [2]. The current situation is further aggravated due to the emergence of multi- and extensively drug-resistant strains and failure of BCG vaccine to impart protection against adulthood TB [1]. However, the combination of phenotypic screening and next generation sequencing has resulted in identification of bedaquiline (BDQ), delamanid and pretomanid (PA-824) that have been approved by FDA for use to treat individuals with MDR-TB [3–8]. Further, resurgence in TB drug discovery have also led to identification of various small molecules that possess a novel mechanism of action and are being evaluated for safety in different stages of clinical trials [9–13].

Thiophene based compounds have been reported to possess antimicrobial, analgesic, anti-inflammatory, antihypertensive and antitumor activity [14–17]. Thiophene based compounds (Fig. 1) have also been reported for their anti-tubercular activity [17–24]. Wilson et al. screened a NIH library of 1113 compounds in *iniBAC* reporter assay and identified two lead compounds **A** and **B** (Fig. 1) having capability to inhibit mycobacterial growth by targeting Pks13 enzyme [18]. In another study, Aggarwal et al. showed that TAM16, a benzofuran scaffold inhibits thioesterase activity associated with Pks13 [23]. A small molecule **C** was identified using NMR based fragment screening of antigen 85C [20]. However the identified molecule possesses weak activity against *M. tuberculosis*. Ibrahim et al. reported that ethyl 2-amino-4,5,6,7-tetrahydrobenzo [b]thiophene-3-carboxylate (compound **D**) inhibits mycolyl transferase activity of Ag85C, however, the lead compound displayed

* Corresponding author.
** Corresponding author.
E-mail addresses: ramandeep@thsti.res.in (R. Singh), dinesh.mahajan@thsti.res.in (D. Mahajan).
[1] Authors contributed equal to the study.

https://doi.org/10.1016/j.ejmech.2020.112772
0223-5234/

MIC_{99} values of 1.8 μM against *M. tuberculosis* in whole cell based assays [21]. In a target-based screening study against tyrosine phosphatase activity of PtpB, thiophenesulfonamide (compound **E**) was identified [22]. In a whole cell based screening against *M. tuberculosis*, another thiophene based compound **F** was identified [19].

In the present study, we are reporting the synthesis and screening of a novel library of thiophene based compounds for activity against *M. tuberculosis*. We have identified few novel compounds that are more potent than INH and also exhibit synergy with BDQ, a recently FDA-approved drug for individuals suffering with MDR-TB. The identified compounds also possess activity against intracellular bacteria in THP-1 macrophages.

2. Results and discussion

The chemical synthesis of various thiophene analogues was performed by diversification of a key intermediate **7**. The synthesis of intermediate **7** was achieved by reaction of ethyl cyanoacetate **6**, with elemental sulfur [S_8] in the presence of 2-phenylacetaldehyde (**5**) under mild condition as mentioned in the Scheme 1 [25]. The intermediate **7** was subsequently derivatized by coupling with different carboxylic acids leading to the synthesis of corresponding amides **1a-h** (Scheme 1). In a typical procedure, the carboxylic acid was activated by methanesulfonyl chloride (MsCl), followed by the addition of intermediate **7** as a solution in dichloromethane (DCM), as mentioned in Scheme 1 (*vide infra*). Additionally, the key intermediate **7** was used for the synthesis of urea derivatives **2a-k.** To achieve this synthesis, **7** was reacted with triphosgene, followed by addition of corresponding amine to form **2a-k** as mentioned in Scheme 2 (*vide infra*).

All newly synthesized molecules of both the series i.e. **1a-h** and **2a-k** were evaluated for whole-cell anti-tubercular activity in triplicates using INH as a positive control. MIC_{99} values were determined against *M. tuberculosis* $H_{37}Rv$ and shown in Table 1 (*vide infra)*. We observed that most of the amide analogues in series **1** (except **1h;** MIC_{99}: 0.78 μM) were unable to inhibit *M. tuberculosis* growth even at 10 μM concentration. However, the screening data of urea analogues of series **2** was encouraging. Three new molecules i.e. **2d**, **2g** and **2h** showed anti-mycobacterial activity in the range of 1.56−3.12 μM. The analysis of activity data of series **1** and **2** provided some intriguing insights on structure activity relationship (SAR). The intermediate **7** itself was observed to be inactive. It was observed that minor modifications in the structures resulted in considerable alteration in anti-mycobacterial activity. For example, compound **2d**, a urea analogue with diethylamine is active (MIC_{99}: 3.12 μM), whereas the associated analogues **2c** (dimethylamine) and **2e** (pyrrolidine) were inactive with MIC_{99}: >10 μM. In concordance, compounds substituted with higher structural homologs of pyrrolidine i.e. piperidine (**2f)** and morpholine (**2j)** were also found to be inactive (MIC_{99}: >10 μM). In continuation, loss of anti-mycobacterial activity was also observed for analogues synthesized from more bulky amines such as aniline and benzylamine i.e. **2k** and **2l** respectively. This data indicates the possibility of steric clashes between target structure and ligands possessing bulky substituents. In contrast, we noticed that the replacement of diethylamine (**2d**; 3.12 μM) with isopropylamine (**2g**; 1.56 μM) at R_2 position resulted in 2.0-fold increase of anti-mycobacterial activity (Table 1). Also, anti-mycobacterial activity of the compounds was retained when isopropylamine **(2g**; 1.56 μM**)** or diethylamine (**2d**; 3.12 μM**)** was replaced with conformationally restricted cyclopropylamine (**2h)**. The synthesized compounds were non-cytotoxic even at 50 μM in our cell viability assays (Table 1). Taken together, SAR understanding from series **1** and **2** suggested that these compounds inhibit bacterial growth by interacting with a specific target. Despite our lack of understanding for the molecular target of this series of compounds, the SAR studies suggested that the anti-tubercular activity is sensitive to the right-hand side derivatization on amine. The *in vitro* anti-tubercular activity was observed to be sensitive for size/steric bulk as well as conformation of the substituents at N-atom. This advocates the presence of a well-defined three-dimensional pocket in the molecular target. Based on these results, we further designed new analogues of the two most active molecules **1h** and **2h** as described in Schemes 3 and 4 (*vide infra*).

The synthesis of second generation analogues was initiated as mentioned in Scheme 3. A suitable protection of methyl 2-aminothiophene-3-carboxylate **(8)** was achieved by utilizing $(Boc)_2O$. Further, the protected intermediate was reacted with *N*-bromosuccinimide to form compound **9** in good yield and purity. The compound **9** was used for the synthesis of two new key intermediates **10** (Scheme 3) and **11** (Scheme 4) which served as precursors for synthesis of **3a-e** and **4a-h**, respectively. The intermediate **10** was reacted with triphosgene and desired amine to get different urea derivatives i.e. **3a-e**. The intermediate **11** was reacted with different acid chlorides to prepare corresponding amides **4a-h**. The compounds **3a-e** and **4a-h** were evaluated for their anti-tubercular activity (Table 2). All newly synthesized urea analogues (**3a-e**) of compound **2h** were found to be inactive. The lack of activity of compounds **3b**, **3c** was explainable based on the structural similarity of these molecules to compounds **2e** and **2f** as mentioned in Table 1. However, the complete loss of activity for compounds **3a**, **3d** and **3e** which are fluorine-substituted derivatives of active compounds **2d**, **2g** and **2h,** respectively was

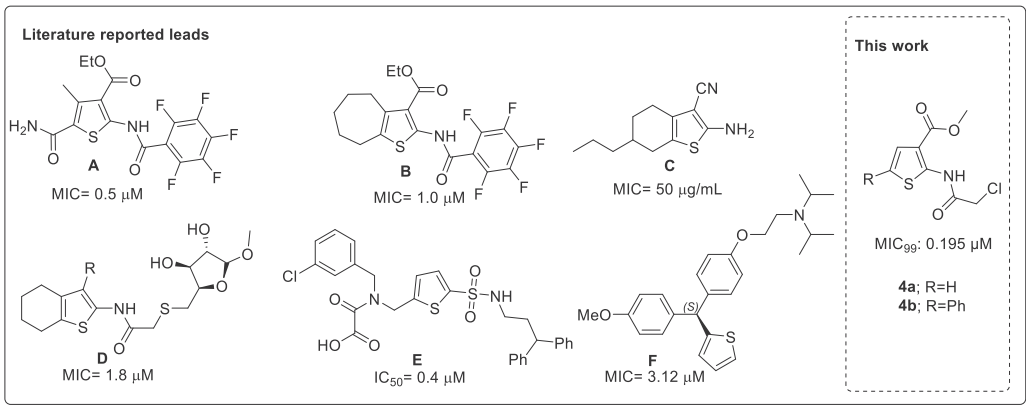

Fig. 1. Reported small molecules based on thiophene scaffold with their anti-tubercular activity.

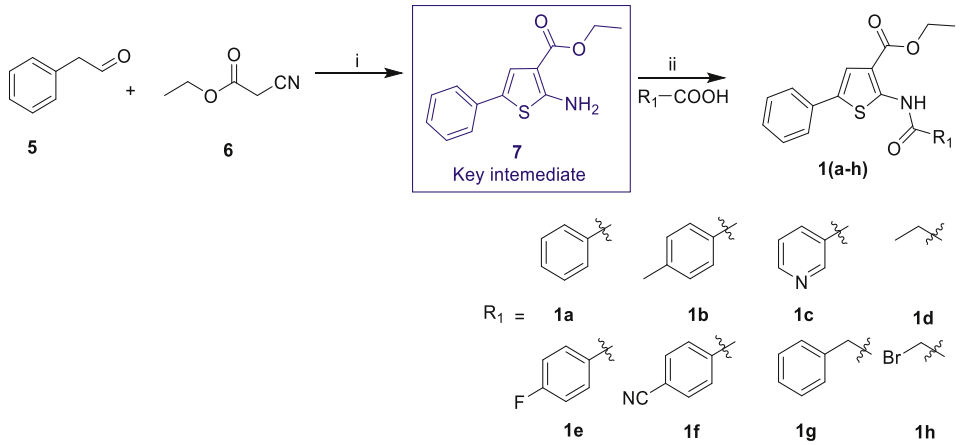

Scheme 1. Reagents and conditions: (i) Et_3N, S_8, EtOH, rt, 24 h (ii) DCM, MsCl, DIPEA, 0 °C to rt, 2 h.

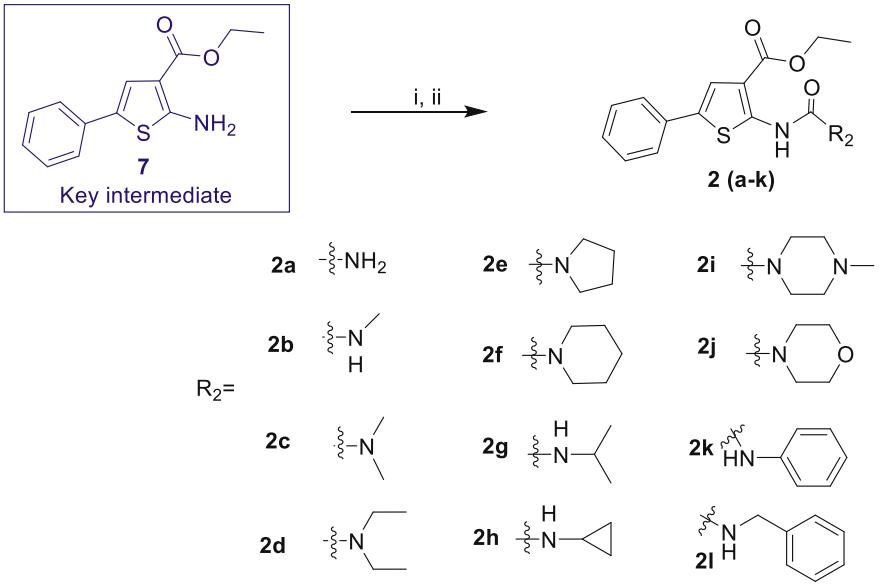

Scheme 2. Reagents and conditions: (i) Triphosgene, Toluene, reflux, 12 h (ii) Desired amine, DIPEA, rt, 2–6 h.

surprising. The fluorine atom has a bigger size (van der Waals radius of 1.47 Å), comparable to hydrogen (van der Waals radius of 1.20 Å), but the associated complete loss of activity was not anticipated owing to such a minor steric perturbation. However, it may not be wise to disregard the contribution of significant change in electronic nature of the molecule due to substitution of fluorine as previously reported [26]. This certainly needs further study for a better understanding. However, we also observed a 4.0-fold increase in potency with the chloro analogue **4a** in comparison to the analogue with bromine substitution, **1h**. This increase in potency instigated to the synthesis of new set of molecules (**4a** and **4c-g**) around **4b** with structural changes on R_1 (Table 2). Unlike urea analogues, the changes on the R_1 position demonstrated very minimal effect on the activity of **4b**. Consistent to earlier findings from data of series 3, flouro substitution demonstrated a detrimental effect on activity (**4b** vs **4c**) in series 4 also. However, this loss was recovered by altering the position of flouro substitution from *-para* to *-meta* (**4c** vs **4d**). In our cell viability experiments, the analogues synthesized in Scheme 3 and Scheme 4 were inactive even at 50 μM concentration (Table 2). In conclusion, the screening of different analogues for anti-mycobacterial activity resulted in identification of four leads **4a**, **4b**, **4d** and **4f** which exhibited better or comparable activity to INH, a first-line TB drug. Since the active compounds **4a-g**, possess electrophilic α-chloroacetamide moiety, so there is a possibility that these molecules inhibit mycobacterial growth by covalently binding to target protein.

Subsequent experiments were performed using **4a** and **4b**, the two most active compounds identified in our screen. We next determined the mode of *M. tuberculosis* killing by selected compounds **4a** and **4b** *in vitro* and in macrophages. As shown in Fig. 2A, we observed that exposure of *M. tuberculosis* early-logarithmic cultures to these compounds at 10x MIC_{99} resulted in growth inhibition. We noticed that in comparison to untreated samples, 10.0-fold less bacterial numbers were observed upon exposure of *M. tuberculosis* to 10x MIC_{99} concentration of both **4a** and **4b** for 7 days (Fig. 2A). As expected, >4 $\log_{10}$ killing was observed upon exposure of early-log phase culture to INH (Fig. 2A). We also determined the ability of both **4a** and **4b** to inhibit growth of intracellular bacteria in THP-1 macrophages. We observed that exposure to **4a** and **4b** for 4 days inhibited the growth of intracellular bacteria by 2.5- and 5-fold, respectively, in THP-1 macrophages (Fig. 2B). As expected, exposure to INH for 4 days inhibited

Table 1
MIC_{99}values of various amides/ureas against *M. tuberculosis* $H_{37}Rv$.

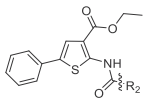

Sr. No	Compound No	R_2	MIC_{99} [μM]	Cytotoxicity [μM]
1	7	NA	>10	>50
2	1a		>10	>50
3	1b		>10	>50
4	1c		>10	>50
5	1d		>10	>50
6	1e		>10	>50
7	1f		>10	>50
8	1g		>10	>50
9	1h		0.78	>50
10	2a		>10	>50
11	2b		>10	>50
12	2c		>10	>50
13	2d		3.12	>50
14	2e		>10	>50
15	2f		>10	>50
16	2g		1.56	>50
17	2h		1.56	>50
18	2i	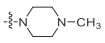	>10	>50
19	2j		>10	>50
20	2k		>10	>50
21	2l	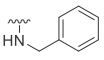	>10	>50
22	INH	–	0.39	>50

the growth of intracellular bacteria by ~200 fold (Fig. 2B).

A new drug lead possessing capability to decrease dosing concentration of existing drugs, when used in combination, can potentially reduce dose associated side effects. Therefore, we determined the activity of **4a, 4b** alone or in combination with RIF, INH, LEVO, BDQ or PA-824 using two-drug checkerboard assay as previously described [27,28]. As shown in Fig. 2C, **4a** and **4b** synergised with BDQ against *M. tuberculosis* with the FICI value of 0.5 and 0.25 respectively. The combination of **4a** and **4b** with BDQ improved their individual MIC_{99} by 4.0-fold and 8.0 fold, respectively (Fig. 2C). We also observed the additive effect of **4a** and **4b** when used in combination with other TB drugs. The FICI values of **4a** and **4b** with RIF were 0.75 and 0.625 with INH were 0.75 and 0.562 and with LEVO were 0.562 and 0.562 and with PA-824 were 1.0 and 0.625, respectively (Fig. 2C). Previously, it has been shown that BDQ shows synergy with drugs involved in lipid transport and arabinan biosynthesis such as BTZ043 and SQ-109 [29,30]. The observed synergy between **4a**, **4b** and BDQ could be attributed to

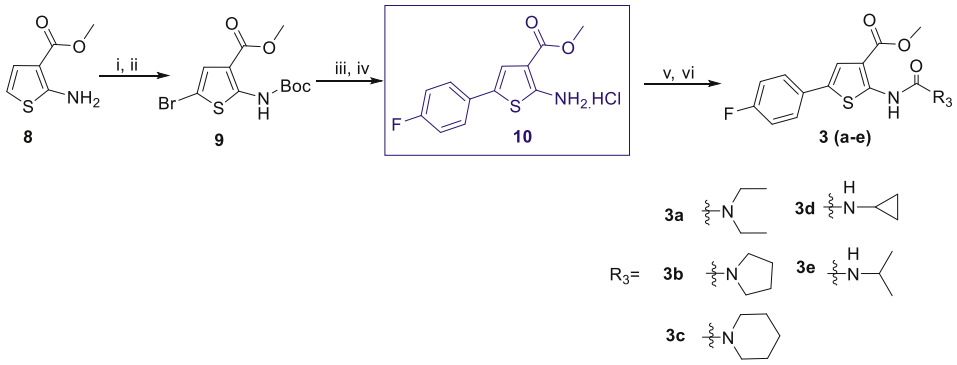

Scheme 3. Reagents and conditions: (i) DCM, $(BOC)_2O$, 4-(Dimethylamino)pyridine, rt, 24h (ii) NBS, AcOH:DCM, (1:1) rt, 3h (iii) 4-Flurophenyl boronic acid, *aq*.K_2CO_3, $Pd(PPh_3)_4$, 1,4-dioxane, N_2(g), 80 °C, 3–4h (iv) *4M* HCl in 1,4-Dioxane, rt (v) Triphosgene, Toluene, reflux, 12 h, (vi) Desired amine, DIPEA, Dry DCM, rt. 2h

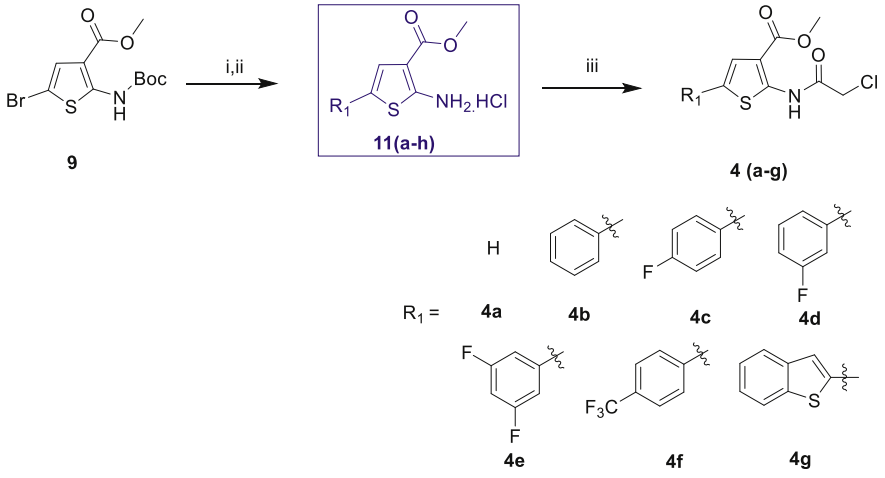

Scheme 4. Reagents and conditions: (i) Ar–$B(OH)_2$, $Pd(PPh_3)_4$, 80 °C, 3–4h (ii). 4M HCl in 1,4-Dioxane (iii) $ClCH_2COOH$., Dry DCM, MsCl, DIPEA, rt, 2h

the fact that these molecules either interact with a complementary off target or facilitate disruption of the cell wall architecture leading to increased BDQ intracellular levels. Taken together, the data presented suggests that the lead molecules have the potential to reduce the dosing concentration of BDQ in clinical settings. The use of combination therapy might result in (i) faster clearance of bacteria (ii) better patient compliance and (iii) minimize the emergence of drug-resistant strains.

It has been shown that the over expression of the drug target involved in mechanism of action may result in resistance to the corresponding drug. An increase in anti-tubercular activity for TB drugs i.e. INH, PZA and cycloserine (CS) have been reported when their corresponding targets *inhA*, *rpsA* and *alrA* have been overexpressed [31–33]. Previous studies have shown that thiophene based scaffolds inhibit mycobacterial Pks13 and an increase in MICs was observed upon overexpression of Pks13 in *M. tuberculosis* [18]. Therefore, the active compounds identified from the present study were further evaluated for their inhibitory activity in Pks13 overexpressing strain of *M. tuberculosis*. We observed that overexpressing of Pks13 did not alter the activity of these analogues; thereby suggesting that Pks13 is not the cellular target for these identified leads (Table 3).

Due to the emergence of drug-resistant strains, there is an urgent need to identify small molecules that possess inhibitory activity against drug-resistant strains. Therefore, we next evaluated the activity of the active compounds against INH resistant *M. tuberculosis* strain, which harbours a mutation in activating enzyme, KatG gene. Previously, it has been reported that *M. tuberculosis* KatG activates the INH by facilitating its hydrolysis [34]. Surprisingly, all active compounds were unable to inhibit the growth of INH resistant strain (Table 3). These observations suggest that KatG is involved in the mechanism of action of these identified drug leads. Since the lead compounds **4a** and **4b** were inactive in resistant strains harbouring mutations in KatG, we performed molecular docking studies to study the interaction of these thiophene analogues with KatG. The interaction maps of compounds **4a** and **4b** with KatG was also compared with the reported interaction map of KatG and INH (Fig. 3). The molecular docking of molecules was performed on the reported crystal structure of KatG (PDB-ID: 1SJ2) [35]. For optimum understanding of the INH binding site as well as key interacting residues, another co-crystal structure i.e. 3WXO was also referred in the present study (Fig. 3A and B). Three binding sites have been reported by Kamachi et al. as potential sites of interactions with INH [36]. We also performed docking of INH in the crystal structure of KatG and observed an overlay between the docked pose with reported co-crystal pose of INH (Fig. 3B). In concordance with previous reports, we found residues W77, W78, K130, L291, W293, I294, N295, G300 and I301 at binding site 2 are the main INH interacting residues (Fig. 3C). Therefore, the docked pose of INH was considered as grid centre to dock compounds **4a** and **4b** at binding site 2. The molecular docking was conducted for all the three reported INH potential interaction sites; however we observed that both the compounds **4a** and **4b** have shown considerably good docking scores at site 2 in comparison to site 1 and site 3. Therefore, only site 2 was considered for further extensive focused docking studies to obtain the most likely

Table 2
MIC_{99}values of compounds against *M. tuberculosis* $H_{37}Rv$.

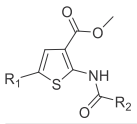

Sr. No	Compound No	R_1	R_2	MIC_{99} [μM]	Cytotoxicity [μM]
23	3a			>10	>50
24	3b			>10	>50
25	3c			>10	>50
26	3d			>10	>50
27	3e			>10	>50
28	4a	H		0.195	>50
29	4b			0.195	>50
30	4c			0.78	>50
31	4d			0.195	>50
32	4e			0.78	>50
33	4f			0.39	>50
34	4g	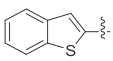		0.78	>50
35	INH	–	–	0.39	>50

orientation of compounds. The docking energy of compound **4b** was −9.3 kcal/mol with 113 conformations and binding free energy (ΔG) of - 54.2 kcal/mol, while the docking energy of compound **4a** was −8.4 kcal/mol with 89 conformations and ΔG = −43.8 kcal/mol. However, the docking energy of INH was found to be −7.2 kcal/mol with 91 conformations along with ΔG = −41.3 kcal/mol. Apart from sharing common INH interacting residues, the compound **4b** was also found to interact with residues N127, L277 G292. Unlike compound **4b,** compound **4a** interacted with residue Q298 only and did not show any interaction with residues K130 and L291 (Fig. 3D and E). This study suggested that the binding site of **4a** and **4b** overlapped with that of INH and these three compounds potentially bind in same orientation. Additionally, for both **4a** and **4b**, the aromatic residues of the binding site appear as the major contributors for net binding affinity followed by hydrophobic contacts. We observed that both the compounds **4a** and **4b** also established the hydrogen bonds (HBs) with key residues. The compound **4a** showed HBs with residues N295 and G300, while compound **4b** formed three HBs with residues N127, K130 and N295. However, no HBs were found in the case of INH. Overall, from this study, it may be concluded that compounds **4a** and **4b** possibly mimic the binding pattern and orientation of INH in KatG for their interactions.

3. Conclusions

In summary, this work led to the identification of a new class of inhibitors that possess potent *in vitro* anti-tubercular activity. Compound **4a** and **4b** were found to be more potent than INH, a first line drug in our MIC_{99} determination assays. The two leads demonstrated additive effect with front line TB drugs (INH, RIF and LEVO) and synergistic effect with a recently approved drug BDQ, when used in combination. The identified compounds were also able to clear the growth of intracellular *M. tuberculosis* in THP-1 macrophages. *In vitro* studies suggest the involvement of KatG in the mechanism of action of **4a** and **4b**.

4. Experimental section

4.1. General methods for the synthesis

Unless otherwise stated, all the chemicals, silica and analytical TLC were purchased from Sigma-Aldrich, Avra Pvt Ltd., Spectrochem and Merck. All intermediates and final compounds were routinely checked for their purity on pre-coated silica gel G254 TLC plates (Merck), Visualization of spot on TLC was achieved by the use of UV light (254 nm) or by iodine vapours. All the synthesized

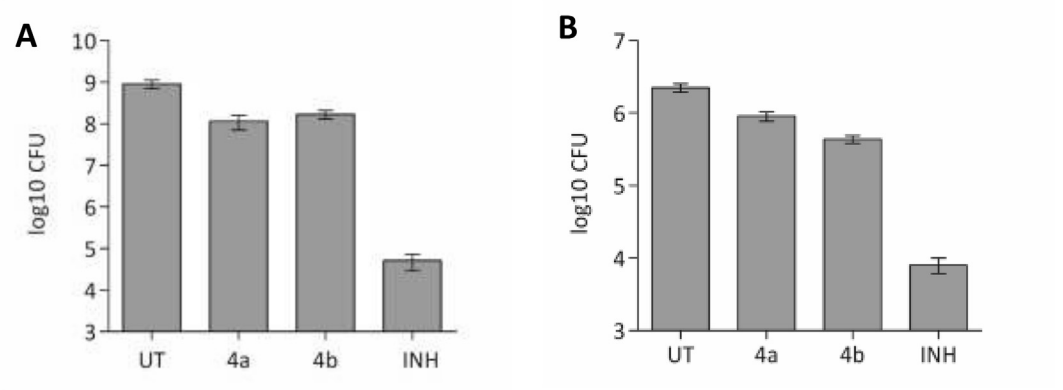

C

Compounds (ID)	Interaction with TB drug (FICI#)				
	Rifampicin	Isoniazid	Levofloxacin	Bedaquiline	Pretomanid
4a	Additive (0.75)	Additive (0.75)	Additive (0.562)	Synergistic (0.5)	Additive (1)
4b	Additive (0.625)	Additive (0.562)	Additive (0.562)	Synergistic (0.25)	Additive (0.625)

#FICI value ≤0.5 indicates synergistic activity, FICI of ≥4.0 indicates antagonistic activity, and values in between ≤ 4.0 and ≥0.5 indicate an additive or indifferent interaction.

Fig. 2. (A) *In vitro* killing of selected hits in liquid cultures. Early-logarithmic phase (OD_{600nm} ~ 0.2) culture of *M. tuberculosis* was exposed to 10x MIC_{99} of various compounds for 7 days followed by CFU enumeration. **(B) Intracellular activity of the selected hits;** THP-1 cells were infected with *M. tuberculosis* followed by treatment with **4a**, **4b** or INH for 4 days. At designated time points, the infected macrophages were lysed with 0.1% PBST. For CFU enumeration, tenfold serial dilutions of the samples were plated on MB 7H11 agar and incubated at 37 °C for 3–4 weeks. **(C) *In vitro* drug combination of selected hits with TB drugs against *M. tuberculosis*.** In order to determine drug-drug interactions, checkerboard assays were performed. Two fold serial dilutions of the lead compounds **4a** and**4b** were prepared horizontally. This was followed by 2.0 fold cross-dilution with TB drugs to make various combinations. FICI values for each combination were calculated as described in Materials and Methods.

Table 3
MIC_{99} of thiophene analogues against parental, Pks13 overexpressing and INH resistant *M. tuberculosis* strains.

Treatment	*M. tuberculosis* wild type	Sensitivity Profile[a]		
		M. tuberculosis-pMV306	*M. tuberculosis*-pMV306-pks13	INH^R-mc^2 497
4f	0.39	S	S	R
4d	0.19	S	S	R
4g	0.78	S	S	R
4c	0.78	S	S	R
4e	0.78	S	S	R
4b	0.19	S	S	R
4a	0.19	S	S	R
1h	0.78	S	S	R
INH	0.19	S	S	R
RIF	0.007	ND[b]	ND	S

[a] In comparison to parental strain, MIC_{99} values of equal to 2x MIC_{99} or less are denoted by S; Sensitive and MIC_{99} values of equals to 4x MIC_{99} or more denoted as R; Resistant.
[b] ND; not done.

compounds were purified on column chromatographic by using of 100–200, 230–400 Mesh Silica gel. Automated flash column chromatography was undertaken on SiO_2 (230–400 mesh). The ^1H and ^{13}C NMR spectra were recorded either using a Bruker Avance DPX 400 (400 MHz for ^1H and 100 MHz for 13C) or Bruker Avance 300 (300 MHz for 1H and 75 MHz for ^{13}C) spectrometer in $CDCl_3$ or DMSO-d_6 using TMS as an internal standard. Proton and carbon chemical shifts are expressed in parts per million (ppm, δ scale) and were reference to NMR solvent $CDCl_3$ δ 7.26, 77 ppm, and DMSO-d_6 δ 2.5, 39.8 ppm respectively. The following abbreviations were used to describe peak patterns when appropriate: bs = broad singlet, s = singlet, d = doublet, t = triplet, q = quartet and m = multiplet. HRMS mass spectra were recorded on a Thermo Scientific Q-Exactive, Accela 1250 pump.

4.1.1. Ethyl 2-amino-5-phenylthiophene-3-carboxylate (**7**)

The mixture of ethyl cyanoacetate (107 mL, 1.0 mol), elemental sulfur (S_8) (32 gm, 1.0 mol) and 2-phenylacetaldehyde (116 mL, 1.0 mol) in ethanol (200 mL) was stirred at room temperature. This was followed by dropwise addition of diethylamine (80 mL) with stirring. The reaction mixture was left at room temperature for 14h; the precipitate was filtered under vacuum, washed by ethanol and dried in air. Yield: 89%; ^1H NMR (300 MHz, DMSO-d_6) δ 7.48–7.44 (m, 4H, Ar–H + NH_2), 7.33 (t, J = 7.8 Hz, 2H, Ar–H), 7.24 (s, 1H, Ar–H), 7.21–7.17 (m, 1H, Ar–H), 4.24–4.19 (m, 2H, CH_2), 1.25–1.30, (m, 3H, CH_3); ^{13}C NMR (75 MHz, $CDCl_3$) δ 165.44, 162.07, 134.00,

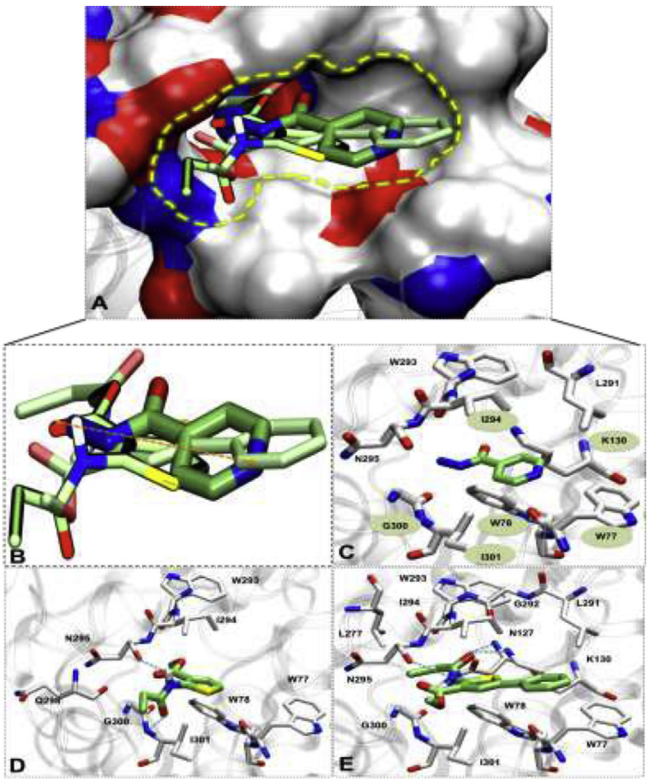

Fig. 3. Interaction map of compounds with *M. tuberculosis* KatG;(A) INH (centred:thick:darkgreen), **4a** (light green) and **4b** (opaque green) are shown in the binding site of *M. tuberculosis* KatG. The binding site is shown in surface view and the molecules are rendered in licorice. **(B)** The zoom-in inset view is highlighting the overlay between INH and compounds **4a** and **4b**. The orange dotted line highlights the alignment of core chemical moiety. **(C)** The interacting residues within 3.5 Å from the centre of the INH (co-crystal pose from PDB ID: 3WXO). The residues of INH binding sites which were reported earlier are highlighted in green circles. **(D and E)** The interacting residues of compound **4a** (D) and **4b** (E) with KatG of *M. tuberculosis* are shown. For the entire image panel the rendering was done as per atom wise like O: red, N: blue, C: green (different shades) and S:yellow. The KatG protein is shown in cartoon and in ghost view. (For interpretation of the references to colour in this figure legend, the reader is referred to the Web version of this article.)

128.92, 126.69, 124.88, 124.71, 121.23, 107.97, 59.90, 14.57; HRMS (ESI-TOF): Calculated *m/z* for $C_{13}H_{13}NO_2S$ 247.0667, found 247.0659.

4.1.2. Ethyl 2-benzamido-5-phenylthiophene-3-carboxylate (*1a*)

To a stirred solution of benzoic acid (244 mg, 1 equiv, 2 mmol) in dry DCM at 0 °C, methanesulfonyl chloride (0.184 mL, 1.2 equiv, 2.4 mmol) and triethylamine (0.612 mL, 2.2 equiv, 4.4 mmol) were added, and stirred for 30 min and followed by addition of intermediate **7** (543 mg, 1.1 equiv, 2.2 mmol) and stirred for 2h at room temperature. The resulting solution was diluted with DCM (20 mL), subsequently washed by *1N* HCl (20 mL), saturated $NaHCO_3$ solution (10 mL) and brine solution (10 mL). Organic layer was separated and dried using anhydrous Na_2SO_4 and concentrated to dry under vacuum. The crude product thus obtained was purified using silica gel column chromatography employing DCM: Hexane (80:20) as eluent. The purified fraction was concentrated under reduced pressure to afford **1a** as a white solid. Yield: 60%; ^{1}H NMR (300 MHz, DMSO-d_6): δ 11.82 (s, 1H, NH), 7.96 (t, J = 2.2 Hz, 2H, Ar−H), 7.69−7.64 (m, 5H, Ar−H), 7.60 (s, 1H, Ar−H), 7.42 (m, 2H, Ar−H), 7.30 (m, 1H, Ar−H), 4.39−4.37 (m, 2H, CH_2), 1.38−1.35 (m, 3H, CH_3), ^{13}C NMR (75 MHz, $CDCl_3$) δ 166.01, 163.58, 148.54, 134.00, 133.78, 132.78, 132.03, 129.05, 128.99, 127.54, 127.49, 125.51, 119.31, 114.10, 61.01, 14.44; HRMS (ESI-TOF): Calculated *m/z* for $C_{20}H_{17}NO_3S$, 351.0929, found, 352.1002 $[M+H]^+$.

4.1.3. Ethyl 2-(4-methylbenzamido)-5-phenylthiophene-3-carboxylate (*1b*)

The synthetic method of **1a** was adopted to synthesize **1b**. Yield: 53%; ^{1}H NMR (400 MHz, DMSO-d_6) δ 11.80 (s, 1H, NH), 7.90 (m, 2H, Ar−H), 7.70 (m, 2H, Ar−H), 7.60 (s, 1H, Ar−H), 7.50−7.40 (m, 5H, Ar−H), 4.38−4.36 (m, 2H, CH_2) 2.43 (s, 3H, CH_3), 1.39 (m, 3H, CH_3), ^{13}C NMR (75 MHz, $CDCl_3$) δ 166.01, 163.58, 148.73, 143.55, 133.83, 129.72, 129.20, 128.98, 127.57, 127.44, 125.49, 119.29, 113.89, 60.97, 21.67, 14.45; HRMS (ESI-TOF): Calculated *m/z* for $C_{21}H_{20}NO_3S$, 366.1164, found 366.1158 $[M+H]^+$.

4.1.4. Ethyl 2-(nicotinamide)-5-phenylthiophene-3-carboxylate (*1c*)

The synthetic method of **1a** was adopted to synthesize **1c**. Yield: 56%; ^{1}H NMR (300 MHz, DMSO-d_6) δ 11.80 (s, 1H, NH), 8.90−9.10 (m, 2H, Ar−H), 8.30 (m, 1H), 7.69 (d, J = 7.2 Hz, 3H, Ar−H), 7.62 (s, 1H, Ar−H), 7.45−7.42 (m, 2H, Ar−H), 7.33 (m, 1H, Ar−H), 4.40−4.38 (m, 2H, CH_2), 1.40−1.36 (m, 3H, CH_3), ^{13}C NMR (75 MHz, $CDCl_3$); 166.02, 161.84, 153.34, 148.93, 147.75, 135.10, 133.56, 129.04, 127.89, 127.60, 125.55, 123.72, 119.31, 114.68, 61.20, 14.41; HRMS (ESI-TOF): Calculated *m/z* for $C_{19}H_{16}N_2O_3S$, 352.0882 found 353.0954 $[M+H]^+$.

4.1.5. Ethyl 2-acetamido-5-phenylthiophene-3-carboxylate (*1d*)

The synthetic method of **1a** was adopted to synthesize **1d**. Yield: 59%; ^{1}H NMR (300 MHz, DMSO-d_6) δ 10.87 (s, 1H, NH), 7.64 (t, J = 4.2 Hz, 2H, Ar−H), 7.52 (s, 1H, CH), 7.41 (t, J = 7.8 Hz, 2H, Ar−H), 7.30 (t, J = 3.4 Hz, 2H, Ar−H), 4.37−4.31 (m, 2H, CH_2), 2.29 (s, 3H, CH_3), 1.37−1.34 (m, 3H, CH_3); ^{13}C NMR (75 MHz, $CDCl_3$); δ 167.07, 165.64, 148.09, 133.75, 133.65, 128.95, 127.43, 125.48, 119.03, 113.37, 60.96, 31.95, 31. 64, 29.72, 23.58, 22.72; HRMS (ESI-TOF): Calculated *m/z* for $C_{15}H_{15}NO_3S$, 289.0773, found 290.0845 $[M+H]^+$ 312.0845 $[M+Na]^+$.

4.1.6. Ethyl 2-(4-fluorobenzamido)-5-phenylthiophene-3-carboxylate (*1e*)

The synthetic method of **1a** was adopted to synthesize **1e**. Yield: 49%; ^{1}H NMR (400 MHz, DMSO-d_6) δ 11.77 (s, 1H, NH), 8.03−8.00 (m, 2H, Ar−H), 7.67 (t, J = 4.2 Hz, 2H, Ar−H), 7.59 (s, 1H, Ar−H), 7.50−7.43 (m, 2H, Ar−H), 7.41−7.40 (m, 2H, CH_2), 7.31 (m, 1H, Ar−H), 4.38−4.36 (m, 2H, CH_2), 1.38−1.34 (m, 3H, CH_3); ^{13}C NMR (75 MHz, $CDCl_3$); δ 165.52 (d, $^1J_{CF}$ = 252.75 Hz), 166.10, 162.47, 148.44, 134.11, 133.70, 130.04 (d, $^3J_{CF}$ = 9.0 Hz), 129.00, 128.28 (d, $^4J_{CF}$ = 3.0 Hz), 127.55, 125.50, 119.27, 116.23 (d, $^2J_{CF}$ = 22.5 Hz), 114.15, 61.08, 14.43; HRMS (ESI-TOF): Calculated *m/z* for $C_{20}H_{16}FNO_3S$, 369.0853, found 370.0909 $[M+H]^+$.

4.1.7. Ethyl 2-(4-cyanobenzamido)-5-phenylthiophene-3-carboxylate (*1f*)

The synthetic method of **1a** was adopted to synthesize **1f**. Yield: 69%; ^{1}H NMR (300 MHz, DMSO-d_6) δ 11.90 (s, 1H, NH), 8.15 (m, 4H, Ar−H), 7.70 (m, 2H, Ar−H), 7.65 (s, 1H, Ar−H), 7.40 (m, 2H, Ar−H), 7.32 (m, 1H, Ar−H), 4.41−4.39 (m, 2H, CH_2), 1.40−1.37 (m, 3H, CH_3); ^{13}C NMR (75 MHz, $CDCl_3$) δ 166.13, 161.59, 147.66, 135.86, 134.78, 133.47, 132.84, 129.06, 128.14, 127.77, 125.56, 119.35, 117.84, 116.19, 114.85, 61.29, 14.41; MS (APCI$^+$): Calculated *m/z* for $C_{21}H_{16}NO_3S$, 377.8, found, 377.9.

4.1.8. Ethyl-5-phenyl-2-(2-phenylacetamido) thiophene-3-carboxylate (*1g*)

The synthetic method of **1a** was adopted to synthesize **1g**. Yield: 62%; ^{1} H NMR (300 MHz, DMSO-d_6) δ 10.87 (s, 1H, NH), 7.64−7.62 (m, 2H, Ar−H), 7.52 (s, 1H, Ar−H), 7.41−7.39 (m, 6H, Ar−H), 7.32 (m, 2H, Ar−H), 4.29−4.27 (m, 2H, CH_2), 3.98 (s, 2H, CH_2), 1.32−1.29,(m,

3H, CH_3), ^{13}C NMR (75 MHz, DMSO-d_6) δ)δ 164.67, 154.02, 151.35, 139.73, 133.93, 130.81, 129.58, 128.90, 127.79, 127.55, 127.48, 125.11, 119.64, 110.64, 60.62, 43.64, 14.78; HRMS (ESI-TOF): Calculated *m/z* for: $C_{21}H_{19}NO_3S$, 366.1158, found 367.1158 $[M+H]^+$.

*4.1.9. Ethyl 2-(2-bromoacetamido)-5-phenylthiophene-3-carboxylate (**1h**)*

The synthetic method of **1a** was adopted to synthesize **1h**. Yield: 53%; ^1H NMR (300 MHz, DMSO-d_6): δ 11.50 (s, 1H, NH), 7.67 (d, J = 7.2 Hz, 2H, Ar−H), 7.59 (s, 1H, Ar−H), 7.43−7.41 (m, 2H, Ar−H), 7.30 (m, 1H, Ar−H), 4.67 (s, 2H, CH_2), 4.37−4.36 (m, 2H, CH_2), 1.37−1.34, (m, 3H, CH_3); ^{13}C NMR (75 MHz, DMSO-d_6); 164.84, 164.53, 164.36, 146.42, 146.26, 133.71, 133.23, 129.69, 128.26, 125.61, 120.03, 115.04, 61.41, 43.00, 29.49, 14.67; HRMS (ESI-TOF): Calculated *m/z* for $C_{15}H_{15}BrNO_3S$, 366.9878, found 367.994 $[M+H]^+$.

*4.1.10. Ethyl 5-phenyl-2-ureidothiophene-3-carboxylate (**2a**)*

To a solution of intermediate **7** (1 gm, 4 mmol, 1.0 equiv.) in toluene, triphosgene (1.26 gm, 4 mmol, 1.05 equiv.) was added and refluxed for 12 h. The mixture was concentrated under vacuum and resulting semisolid residue was used for the next step without purification. The residue (0.2 gm, 0.490 mmol, 1equiv.) was dissolved in dry DCM followed by addition of DIPEA (0.255 mL, 1.47 mmol, 3.0 equiv.) and ammonium hydroxide solution (1.5 mL) and stirred for 2−6 h at room temperature. The reaction mixture was diluted with DCM (20 mL) and subsequently washed by diluted HCl, followed by saturated $NaHCO_3$ solution. The organic layer was dried over anhydrous Na_2SO_4 and concentrated under vacuum. The residue was purified by column chromatography using DCM: hexane (90:20) as eluent, resulting in **2a** as a white solid**.** Yield: 91%; ^1H NMR (300 MHz, DMSO-d_6) δ 10.18 (s, 1H, NH), 7.59 (d, J = 7.2 Hz, 2H, Ar−H), 7.42 (s, 1H, Ar−H), 7.40−7.36 (m, 2H, Ar−H), 7.28−7.24, (m, 1H, Ar−H), 7.20 (bs, 1H, NH), 4.34−4.29 (m, 2H, CH_2), 1.35−1.32 (m, 2H, CH_2); ^{13}C NMR (75 MHz, DMSO-d_6) δ 164.69, 164.65, 154.76, 154.72, 154.68, 151.52, 151.36, 133.95, 130.92, 129.57, 127.52, 125.13, 119.55, 110.55, 100.00, 60.60, 14.77; HRMS (ESI-TOF): Calculated *m/z* for $C_{14}H_{14}N_2O_3S$ 291.0725, found 291.0843$[M+H]^+$.

*4.1.11. Ethyl 2-(3-methylureido)-5-phenylthiophene-3-carboxylate (**2b**)*

The synthetic method of **2a** was adopted to synthesize **2b**. Yield: 73%; ^1H NMR (400 MHz, DMSO-d_6) δ 10.20 (s, 1H, NH), 7.80 (bs, 1H, NH), 7.65−0.760 (m, 2H, Ar−H), 7.41 (m, 3H, Ar−H), 7.24−7.20 (m, 1H, Ar−H), 4.32−4.30 (m, 2H, CH_2), 2.71 (d, J = 4.8 Hz, 3H, CH_3), 1.35−1.33, (m, 3H, CH_3); ^{13}C NMR (75 MHz, $CDCl_3$) δ 166.04, 154.26, 151.67, 134.02, 131.96, 128.90, 127.08, 125.19, 119.00, 111.03, 60.59, 27.37, 14.42; HRMS (ESI-TOF): Calculated *m/z* for $C_{15}H_{17}N_2O_3S$ 304.0882, found 305.0950 $[M+H]^+$, 327.0769 $[M+Na]^+$.

*4.1.12. Ethyl 2-(3, 3-dimethylureido)-5-phenylthiophene-3-carboxylate (**2c**)*

The synthetic method of **2a** was adopted to synthesize **2c**. Yield: 45%; ^1H NMR (300 MHz, DMSO-d_6) δ 10.50 (s, 1H, NH), 7.58 (d, J = 7.6 Hz, 2H, Ar−H), 7.44 (s, 1H, Ar−H), 7.38−7.36 (m, 2H, Ar−H), 7.23−7.20 (m, 1H, Ar−H), 4.32−4.30 (m, 2H, CH_2), 2.99 (s, 6H, $2CH_3$), 1.34−1.30, (m, 3H, CH_3); ^{13}C NMR (75 MHz, DMSO-d_6) δ 165.55, 153.42, 151.76, 133.82, 131.28, 131.28, 129.59, 127.65, 125.16, 119.46, 111.12, 61.00, 36.19, 14,70; HRMS (ESI-TOF): Calculated *m/z* for $C_{16}H_{18}N_2O_3S$, 318.1038, found, 319.1111 $[M+H]^+$.

*4.1.13. Ethyl 2-(3, 3-diethylureido)-5-phenylthiophene-3-carboxylate (**2d**)*

The synthetic method of **2a** was adopted to synthesize **2d**. Yield: 71%; ^1H NMR (300 MHz, $CDCl_3$) δ 10.77 (s, 1H, NH), 7.60 (t, J = 4.5 Hz, 2H, Ar−H), 7.40−7.35 (m, 3H, Ar−H), 7.28−7.23 (m, 1H, Ar−H), 4.41−4.34 (m, 2H, CH_2), 3.51−3.44 (m, 4H, $2CH_2$), 1.45−1.40 (m, 3H, CH_3), 1.33−1.28 (m, 6H, $2CH_3$), ^{13}C NMR (75 MHz, $CDCl_3$) δ 166.27, 152.94, 152.31, 134.19, 131.87, 131.87, 128.86, 126.95, 126.95, 125.15, 118.97, 111.04, 60.55, 41.88, 14.45, 13.70; HRMS (ESI-TOF): Calculated *m/z* for: $C_{18}H_{22}N_2O_3S$, 346.1351 found, 347.1424 $[M+H]^+$.

*4.1.14. Ethyl 5-phenyl-2-(pyrrolidine-1-carboxamido) thiophene-3-carboxylate (**2e**)*

The synthetic method of **2a** was adopted to synthesize **2e**. Yield: 92%; ^1H NMR (300 MHz, DMSO-d_6) δ 10.31 (s, 1H, NH), 7.60 (t, J = 4.2 Hz, 2H, Ar−H), 7.46 (s, 1H, Ar−H), 7.39 (t, J = 7.5 Hz, 2H, Ar−H), 7.30−7.27 (m, 1H, Ar−H), 4.33−4.31 (m, 2H, CH_2), 3.40 (s, 4H, $2CH_2$), 2.00 (s, 4H, $2CH_2$), 1.36−1.31 (m, 3H, CH_3), ^{13}C NMR (75 MHz, $CDCl_3$) δ 166.24, 152.07, 134.16, 131.88, 128.87, 126.98, 125.17, 118.92, 111.01, 60.55, 45.78, 29.71, 14.46; HRMS (ESI-TOF): Calculated *m/z* for $C_{18}H_{20}N_2O_3S$, 344.1195, found, 345.1267 $[M+H]^+$.

*4.1.15. Ethyl 5-phenyl-2-(piperidine-1-carboxamido) thiophene-3-carboxylate (**2f**)*

The synthetic method of **2a** was adopted to synthesize **2f**. Yield: 83%; ^1H NMR (300 MHz, DMSO-d_6) δ 10.65 (s, 1H, NH),7.62−7.59 (m, 2H, Ar−H), 7.47 (s, 1H, Ar−H), 7.39 (t, J = 7.5 Hz, 2H, Ar−H), 7.30−7.28 (m, 1H, Ar−H), 4.34−4.32 (m, 2H, CH_2), 3.46−3.42 (bs, 4H, $2CH_2$), 1.59 (bs, 6H, $3CH_2$), 1.36−1.31 (m, 3H, CH_3), ^{13}C NMR (75 MHz, $CDCl_3$) δ 166.38, 152.79, 152.46, 134.16, 132.03, 128.96, 128.87, 126.98, 125.33, 118.99, 111.04, 60.59, 45.08, 25.68, 24.25, 14.45; HRMS (ESI-TOF) Calculated *m/z* for $C_{19}H_{22}N_2O_3S$, 358.1351 found, 359.1424 $[M+H]^+$.

*4.1.16. Ethyl 2-(3-isopropylureido)-5-phenylthiophene-3-carboxylate (**2g**)*

The synthetic method of **2a** was adopted to synthesize **2g**. Yield: 51%; ^1H NMR (300 MHz, DMSO-d_6) δ 10.14 (s, 1H, NH), 7.95−7.92 (bs, 1H, NH), 7.59−7.57 (m, 2H, Ar−H), 7.41−7.36 (m, 3H, Ar−H), 7.38−7.36 (m, 1H, Ar−H), 7.28−7.23 (t, 2H, Ar−H), 4.34−4.27 (m, 2H, CH_2), 3.76 (m, 1H, CH), 1.33 (m, 3H, CH_3), 1.12 (d, J = 6.6 Hz, 6H, $3CH_3$); ^{13}C NMR (75 MHz, $CDCl_3$) δ 166.09, 152.64, 151.69, 134.06, 131.93, 128.87, 127.03, 125.18, 118.95, 110.91, 60.57, 43.04, 23.16, 14.42; HRMS (ESI-TOF); Calculated *m/z* for $C_{17}H_{20}N_2O_3S$, 332.1195, found 333.1262 $[M+H]^+$ 355.1083 $(M + Na)^+$.

*4.1.17. Ethyl 2-(3-cyclopropylureido)-5-phenylthiophene-3-carboxylate (**2h**)*

The synthetic method of **2a** was adopted to synthesize **2h**. Yield: 81%; ^1H NMR (300 MHz, DMSO-d_6) δ 10.18 (s, 1H, NH), 8.09 (s, 1H, NH), 7.60−7.58 (m, 2H, Ar−H), 7.43 (m, 3H, Ar−H), 7.29−7.27 (m, 1H, Ar−H), 4.35−4.28 (m, 2H, CH_2), 2.62 (m, 1H, CH), 1.35−1.30 (m, 3H, CH_3), 0.40−0.80 (bs, 4H, $2CH_2$); ^{13}C NMR (75 MHz, $CDCl_3$) δ 165.83, 155.00, 150.93, 134.05, 132.35, 128.88, 127.10, 125.26, 119.14, 111.90, 60.54, 22.56, 14.46, 7.71; HRMS (ESI-TOF): Calculated *m/z* for $C_{17}H_{18}N_2O_3S$, 330.1038 found, 331.1111$[M+H]^+$ 353.0922 $[M+Na]^+$.

*4.1.18. Ethyl 2-(4-methylpiperazine-1-carboxamido)-5-phenylthiophene-3-carboxylate (**2i**)*

The synthetic method of **2a** was adopted to synthesize **2i**. Yield: 70%; ^1H NMR (400 MHz, DMSO-d_6) δ 10.63 (s, 1H, NH), 7.61 (t, J = 4.2 Hz, 2H, Ar−H), 7.47 (s, 1H, Ar−H), 7.42−7.38 (m, 2H, Ar−H), 7.30−7.26 (m, 1H, Ar−H), 4.36−4.30 (m, 2H, CH_2), 3.47−3.44 (m, 4H, $2CH_2$), 2.40, (t, 4H, $2CH_2$), 2.09 (s, 3H, CH_3), 1.36−1.32, (m, 3H, CH_3); ^{13}C NMR (75 MHz, DMSO-d_6) δ 165.60, 152.52, 151.50, 133.76, 131.60, 131,60, 129.61, 127.73, 125.21, 119.56, 111.43, 61.09, 61.09, 54.40, 46.07, 43.80, 14.70; HRMS (ESI-TOF): Calculated *m/z* for $C_{19}H_{23}N_3O_3S$, 373.1460 found, 374.1533 $[M+H]^+$.

*4.1.19. Ethyl 2-(morpholine-4-carboxamido)-5-phenylthiophene-3-carboxylate (**2j**)*

The synthetic method of **2a** was adopted to synthesize **2j**. Yield: 83%; ^{1}H NMR (400 MHz, DMSO-d_6) δ 10.57 (s, 1H, NH), 7.57 (d, J = 7.6 Hz, 2H, Ar−H), 7.44 (s, 1H, Ar−H), 7.38−7.34 (m, 2H, Ar−H), 7.26−7.24 (m, 1H, Ar−H), 4.32−4.26 (m, 2H, CH_2), 3.65−3.63, (m, 4H, $2CH_2$), 3.42−3.40, (m, 4H, $2CH_2$), 1.32−1.28 (m, 3H, CH_3), ^{13}C NMR (75 MHz, $CDCl_3$) δ 166.47, 152.99, 151.75, 133.96, 132.44, 128.92, 127.17, 125.23, 118.99, 111.54, 66.41, 60.77, 43.98, 14.44; HRMS (ESI-TOF): Calculated m/z for $C_{18}H_{20}N_2O_4S$, 360.1144 found, 361.1217 $[M+H]^+$.

*4.1.20. Ethyl 5-phenyl-2-(3-phenylureido) thiophene-3-carboxylate (**2k**)*

The synthetic method of **2a** was adopted to synthesize **2k**. Yield:85%; ^{1}H NMR (400 MHz, DMSO-d_6) δ 10.53 (s, 1H, NH), 10.32 (s, 1H, NH), 7.60 (d, J = 7.2 Hz, 2H, Ar−H), 7.51−7.46 (m, 2H, Ar−H), 7.46−7.40 (m, 2H, Ar−H), 7.33−7.26 (m, 4H, Ar−H), 7.03 (m, 1H, Ar−H), 4.34−4.32 (m, 2H, CH_2), 1.35−1.32 (m, 3H, CH_3); ^{13}C NMR (75 MHz, DMSO-d_6) δ 164.79, 151.45, 150.38, 139.33, 133.79, 131.50, 129.62, 129.45, 127.70, 125.21, 123.25, 119.69, 118.90, 111.48, 60.90, 14.77; HRMS (ESI-TOF): Calculated m/z for $C_{20}H_{18}N_2O_3S$, 366.1038, found, 367.1111 $[M+H]^+$ 389.0930 $[M+Na]^+$.

*4.1.21. Ethyl 2-(3-benzylureido)-5-phenylthiophene-3-carboxylate (**2l**)*

The synthetic method of **2a** was adopted to synthesize **2l**. Yield: 62%; ^{1}H NMR (400 MHz, DMSO-d_6) δ 10.30 (bs, 1H, NH), 8.50 (bs, 1H, NH), 7.59 (t, J = 4.2 Hz, 2H, Ar−H), 7.43 (s, 1H, Ar−H), 7.41−7.32 (m, 6H, Ar−H), 7.28−7.26 (m, 2H, Ar−H), 4.37−4.30 (m, 4H, $2CH_2$), 1.35−1.31, (m, 3H, CH_3); ^{13}C NMR (75 MHz, DMSO-d_6) δ 164.67, 154.02, 151.35, 139.73, 133.93, 130.81, 129.58, 128.90, 127.79, 127.55, 127.48, 125.11, 119.64, 110.64, 60.62, 43.64, 14.70. HRMS (ESI-TOF): Calculated for $C_{21}H_{20}N_2O_3S$, 380.1195, found, 381.1267 $[M+H]^+$ 391.1087$[M+Na]^+$.

*4.1.22. Methyl 2-(3, 3-diethylureido)-5-(4-fluorophenyl) thiophene-3-carboxylate (**3a**)*

To a stirred solution of intermediate **10** (1 gm, 3.98 mmol, 1equiv.) in toluene, triphosgene (1.23 gm, 4.18 mmol, 1.05 equiv.) was added and refluxed for 12 h. The solvent was concentrated under vacuum and resulting residue was used for the next synthetic step without any purification. This residue (0.2 gm, 0.487 mmol, 1 equiv.) was dissolved in dry DCM and DIPEA (0.254 mL, 1.46 mmol, 3equiv.) was added followed by diethylamine (0.071 mL, 0.975 mmol, 2equiv.) and stirred for 2−6 h at room temperature. The reaction mixture was diluted with DCM (20 mL) and subsequently washed with diluted HCl and saturated, $NaHCO_3$ solution. Organic layer was separated and dried using anhydrous Na_2SO_4 and concentrated under vacuum. The resulting residue was purified by column chromatography using DCM: hexane (90:20) as eluent resulting in **3a** as a white solid**.** Yield: 70%; ^{1}H NMR (300 MHz, DMSO-d_6) δ 10.55 (bs, 1H, NH), 7.66−7.61 (m, 2H, Ar−H), 7.44 (s, 1H, Ar−H), 7.25−7.19 (m, 2H, Ar−H), 3.85 (s, 3H, CH_3), 3.41−3.36 (m, 4H, $2CH_2$), 1.23−1.15 (s, 6H, $2CH_3$); ^{13}C NMR (75 MHz, $CDCl_3$) δ 166.58, 162.02 (d, $^1J_{CF}$ = 245.25 Hz), 152.89, 152.40, 130.97, 130.4 (d, $^4J_{CF}$ = 3.0 Hz), 126.78 (d, $^3J_{CF}$ = 8.25 Hz), 118.76, 115.83 (d, $^2J_{CF}$ = 21.0 Hz), 110.65, 51.66, 48.38, 41.91, 29.70, 14.99, 13.68; HRMS (ESI-TOF): Calculated m/z for: $C_{17}H_{19}FN_2O_3S$, 350.1100 found, 351.1173 $[M+H]^+$.

*4.1.23. Methyl 5-(4-fluorophenyl)-2-(pyrrolidine-1-carboxamido) thiophene-3-carboxylate (**3b**)*

The synthetic method of **3a** was adopted to synthesize **3b**. Yield: 86%; ^{1}H NMR (300 MHz, DMSO-d_6) δ 10.30 (s, 1H, NH), 7.65−7.60 (m, 2H, Ar−H), 7.43 (s, 1H, Ar−H), 7.24−7.18 (m, 2H, Ar−H), 3.83 (s, 3H, CH_3), 3.25−3.20 (m, 4H, $2CH_2$), 1.90 (m, 4H, $2CH_2$); ^{13}C NMR (75 MHz, $CDCl_3$) δ 166.56, 162.03 (d, $^1J_{CF}$ = 245.25 Hz), 152.15, 152.01, 130.97, 130.37 (d, $^4J_{CF}$ = 3.0 Hz), 126.81 (d, $^3J_{CF}$ = 8.25 Hz), 118.72, 115.83 (d, $^2J_{CF}$ = 21.0 Hz), 110.62, 51.62, 50.81, 45.82, 25.34, 23.74; HRMS (ESI-TOF): Calculated m/z for $C_{17}H_{17}FN_2O_3S$ 348.0944, found, 349.1017 $[M+H]^+$.

*4.1.24. Methyl 5-(4-fluorophenyl)-2-(piperidine-1-carboxamido) thiophene-3-carboxylate (**3c**)*

The synthetic method of **3a** was adopted to synthesize **3c**. Yield: 72%; ^{1}H NMR (300 MHz, DMSO-d_6) δ 10.63 (s, 1H, NH), 7.64−759 (m, 2H, Ar−H), 7.41 (s, 1H, Ar−H), 7.23−7.17 (m, 2H, Ar−H), 3.83 (s, 3H, CH_3), 3.43−3.42, (m, 4H, $2CH_2$), 1.56 (s, 6H, $3CH_2$); ^{13}C NMR (75 MHz, DMSO-d_6); δ166.12, 160.00, 152.23, 151.98, 130.46, 127.23 (d, $^3J_{CF}$ = 8.25 Hz), 119.53, 116.46 (d, $^2J_{CF}$ = 21.0 Hz), 110.84, 52.35, 44.95, 25.59, 24.06; HRMS (ESI-TOF): Calculated m/z for: $C_{18}H_{19}FN_2O_3S$, 362.1100, found, 363.1173 $[M+H]^+$.

*4.1.25. Methyl 2-(3-cyclopropylureido)-5-(4-fluorophenyl) thiophene-3-carboxylate (**3d**)*

The synthetic method of **3a** was adopted to synthesize **3d**. Yield: 82%; (^{1}H NMR (300 MHz, DMSO-d_6) δ 10.07 (bs, 1H, NH), 8.10 (bs, 1H, NH), 7.65−7.60 (m, 2H, Ar−H), 7.41 (s, 1H, Ar−H), 7.24−7.18 (m, 2H, Ar−H), 3.82 (s, 3H, CH_3), 2.60 (m, 1H, CH), 0.69 (m, 2H, CH_2), 0.45 (m, 2H, CH_2); ^{13}C NMR (75 MHz, DMSO-d_6); δ 161.78 ($^1J_{CF}$ = 242.25 Hz), 154.70, 151.13, 130.48, 127.18 (d, $^3J_{CF}$ = 8.25 Hz), 119.69, 116.45 (d, $^2J_{CF}$ = 21.75 Hz), 52.03, 29.42, 6.63; HRMS (ESI-TOF): Calculated m/z for $C_{16}H_{15}FN_2O_3S$, 334.0787, found 335.0.860 $[M+H]^+$.

*4.1.26. Methyl 5-(4-fluorophenyl)-2-(3-isopropylureido)thiophene-3-carboxylate (**3e**)*

The synthetic method of **3a** was adopted to synthesize **3e.** Yield: 91%; ^{1}H NMR (300 MHz, DMSO-d_6) δ 10.07 (s, 1H, NH), 7.94 (m, 1H, NH), 7.91−7.59 (m, 2H, Ar−H), 7.38 (s, 1H, Ar−H), 7.23−7.18 (m, 2H, Ar−H), 3.89 (s, 3H, CH_3), 3.79−3.73 (bs, 1H, CH), 1.11 (d, J = 6.6 Hz, 6H, $2CH_3$); ^{13}C NMR (75 MHz, $CDCl_3$); δ 166.35, 162.06 (d, $^1J_{CF}$ = 244.5 Hz), 152.61, 151.71, 131.02, 130.26 (d, $^4J_{CF}$ = 3.75 Hz), 126.82 (d, $^3J_{CF}$ = 8.25 Hz), 118.80, 115.84 (d, $^2J_{CF}$ = 21.75 Hz), 110.55, 51.63, 43.08, 23.14; HRMS (ESI-TOF):Calculated m/z for $C_{16}H_{17}FN_2O_3S$, 336.0944, found, 337.1017$[M+H]^+$ 359.0836 $[M+Na]^+$.

*4.1.27. Methyl 2-(2-chloroacetamido) thiophene-3-carboxylate (**4a**)*

To a solution of 2-chloroacetic acid (0.1 g, 1.07 mmol, 1equiv.) in dry DCM (10 mL), a solution of methanesulfonyl chloride (0.099 mL, 1.29 mmol, 1.2 equiv. in 2 mL dry DCM) and triethylamine (0.329 mL, 2.36 mmol, 2.2 equiv) was added at 0 °C. The reaction temperature was maintained and stirred for 30 min. This was followed by an addition of methyl 2-aminothiophene-3-carboxylate **8** (184 mg, 1.18 mmol, 1.2 equiv.). The reaction mixture was stirred further at room temperature for additional 2h and progress of the reaction was monitored by TLC. The reaction was diluted with DCM and subsequently washed with brine solution, dried over anhydrous Na_2SO_4 and concentrated under vacuum to obtain crude product. The crude product was purified by column chromatography using DCM: Hexane (80:20) as eluent to afford **4a** as a white solid. Yield: 54%;^{1}H NMR (400 MHz, DMSO-d_6) δ 11.50 (s, 1H, NH), 7.23 (d, J = 5.6 Hz, 1H, CH), 7.12 (d, J = 5.6 Hz, 1H, CH), 4.64 (s, 2H, CH_2), 3.86 (s, 3H, CH_3); ^{13}C NMR (75 MHz, $CDCl_3$) δ 165.70, 163.69, 147.42, 124.06, 116.92, 114.09, 52.00, 42.16, 29.70; MS ($APCI^+$): Calculated m/z for $C_8H_9ClNO_3S$ 233.999, found 233.9.

*4.1.28. Methyl 2-(2-chloroacetamido)-5-phenylthiophene-3-carboxylate (**4b**)*

Yield: 67%; The synthetic method of **4a** was adopted to synthesize **4b:** ^{1}H NMR (300 MHz, DMSO-d_6) δ 11.50 (bs, 1H, NH), 7.70 (m, 2H, Ar−H), 7.60 (s, 1H, Ar−H), 7.40 (m, 2H, Ar−H), 7.30 (m, 1H, Ar−H), 4.64 (s, 2H, CH_2), 3.86 (s, 3H, CH_3); ^{13}C NMR (75 MHz, $CDCl_3$) δ 165.62, 163.68, 146.54, 134.79, 133.41, 129.02, 127.74, 125.56, 119.31, 114.85, 52.08, 42.16, 40.49, 29.71. HRMS (ESI-TOF): Calculated *m/z* for $C_{14}H_{12}ClNO_3S$, 309.0226 found, 310.0295 $[M+H]^+$ 332.0119 $[M+Na]^+$.

*4.1.29. Methyl 2-(2-chloroacetamido)-5-(4-fluorophenyl) thiophene-3-carboxylate (**4c**)*

The synthetic method of **4a** was adopted to synthesize **4c.** Yield: 63% ^{1}H NMR (400 MHz, DMSO-d_6) δ 11.52 (s, 1H, NH), 7.74−7.70 (m, 2H, Ar−H), 7.58 (s, 1H, Ar−H), 7.27−7.23 (m, 2H, Ar−H), 4.67 (s, 2H, CH_2), 3.89 (s, 3H, CH_3); ^{13}C NMR (75 MHz, $CDCl_3$) δ 165.55, 163.69, 160.80, 146.49, 139.30, 135.06, 133.71, 129.69 (d, $^4J_{CF} = 3.0$ Hz), 127.3 (d, $^3J_{CF} = 7.5$ Hz), 119.29, 116.03 (d, $^2J_{CF} = 21.75$ Hz), 114.84, 52.10, 42.14, 33.41, 31.94; HRMS (ESI-TOF): Calculated *m/z* for $C_{14}H_{11}ClNO_3S$, 328.0132 found 327.0205. $[M+H]^+$ 350.0024 $[M+Na]^+$.

*4.1.30. Methyl 2-(2-chloroacetamido)-5-(3-fluorophenyl) thiophene-3-carboxylate (**4d**)*

The synthetic method of **4a** was adopted to synthesize **4d**. Yield: 56% ^{1}H NMR (300 MHz, DMSO-d_6) δ 11.50 (s, 1H, NH), 7.72 (s, 1H, Ar−H), 7.60−7.58 (m, 1H, Ar−H), 7.50−7.43 (m, 2H, Ar−H), 7.17−7.13 (m, 1H, Ar−H), 4.68 (s, 2H, CH_2), 3.90 (s, 3H, CH_3); ^{13}C NMR (75 MHz, $CDCl_3$) δ 165.49, 163.76, 163.16 (d, $^1J_{CF} = 245.25$ Hz), 146.91, 135.61, 133.27, 130.64, 121.23, 114.85, 112.52, 52.14, 42.14, 29.53, 22.71; HRMS (ESI-TOF): Calculated *m/z* for $C_{14}H_{11}ClNO_3S$, 328.0132 found 327.0202. $[M+H]^+$ 350.0022 $[M+Na]^+$.

*4.1.31. Methyl 2-(2-chloroacetamido)-5-(3, 5-difluorophenyl) thiophene-3-carboxylate (**4e**)*

The synthetic method of 4a was adopted to synthesize **4e**. Yield: 77%; ^{1}H NMR (400 MHz, DMSO-d_6) δ 11.53 (s, 1H, NH), 7.79 (s, 1H, Ar−H), 7.46−7.40 (m, 2H, Ar−H), 7.17−7.11 (m, 1H, Ar−H), 4.67 (s, 2H, CH_2) 3.86 (s, 3H, CH_3); ^{13}C NMR (75 MHz, $CDCl_3$) δ 165.14, 163.86, 147.26, 136.54, 121.02, 114.89, 108.53, 103.21, 102.87, 102.53, 52.21, 42.10, 31.94, 29.71. HRMS (ESI-TOF): Calculated *m/z* for $C_{14}H_{10}ClF_2NO_3S$, 345.0038 found 345.0012 $[M+H]^+$, 367.9932 $[M+Na]^+$.

*4.1.32. Methyl 2-(2-chloroacetamido)-5-(4-(trifluoromethyl) phenyl) thiophene-3-carboxylate (**4f**)*

The synthetic method of **4a** was adopted to synthesize **4f**. Yield: 63%; ^{1}H NMR (300 MHz, DMSO-d_6) δ 11.57 (s, 1H, NH), 7.91 (d, J = 8.0 Hz, 2H, Ar−H), 7.80 (s, 1H, Ar−H), 7.75 (d, J = 8.4 Hz, 2H, Ar−H), 4.69 (s, 2H, CH_2), 3.91 (s, 3H, CH_3); ^{13}C NMR (75 MHz, $CDCl_3$) δ 165.41, 163.87, 147.37, 136.87, 132.81, 129.64, 126.04, 125.99, 122.24, 120.93, 115.03, 52.20, 42.12, 29.71; HRMS (ESI-TOF): Calculated *m/z* for $C_{15}H_{11}ClF_3NO_3S$, 377.0100 found, 378.0172 $[M+H]^+$ 399.9992 $[M+Na]^+$

*4.1.33. Methyl 5-(benzo[b]thiophen-2-yl)-2-(2-chloroacetamido) thiophene-3-carboxylate (**4g**)*

The synthetic method of **4a** was adopted to synthesize **4g.** Yield: 96%; ^{1}H NMR (300 MHz, DMSO-d_6) δ 11.50 (s, 1H, NH), 7.90 (m, 1H, Ar−H), 7.80 (m, 1H, Ar−H),7.70 (s, 1H, Ar−H), 7.40 (s, 1H, Ar−H), 7.30 (m, 2H, Ar−H), 4.71−4.69 (s, 2H, CH_2), 3.89 (s, 3H, CH_3); ^{13}C NMR (75 MHz, $CDCl_3$) δ165.37, 163.80, 146.80, 140.26, 138.99, 136.23, 128.31, 124.82, 124.69, 123.53, 122.11, 121.19, 114.5, 52.19, 42.11, 29.72, 22.72; MS ($APCI^+$): Calculated *m/z* for $C_{16}H_{12}ClNO_3S_2$, 364.99 found 365.85.

4.2. MIC_{99} determination assays

Mycobacterium tuberculosis $H_{37}R_v$ (*M. tuberculosis*) was cultured in Middlebrook 7H9 broth (MB broth) supplemented with 0.05% Tween-80, 0.2% glycerol and 1x albumin-dextrose-saline (ADS) at 37 °C with shaking (200 rpm). MIC_{99} determination assays, two-drug checkerboard assays and *in vitro* killing experiments were performed as previously described [28,37].

4.3. Cell viability experiments

Briefly, THP-1 cells were seeded in 96 well cell culture plates at the density of 20,000/well in the presence of 20 ng/ml of phorbol 12-myristate-13-acetate (PMA). Following 48 h incubation, cells were washed with 1x PBS and overlaid for 24 h in RPMI complete medium (with 10% FBS). The drug dilutions were prepared in RPMI complete medium and added to the designated wells in triplicates. After 96 h of incubation, water soluble tetrazolium salt (WST)-1 cell proliferation reagent was added to each well following incubation for 30 min. Absorbance were taken at 450 nm and 630 nm and % cell viability following drug treatment was calculated as per manufacturer's recommendations.

4.4. Macrophage CFU determination experiments

THP-1 cells (human monocytic cell line) were cultured in RPMI medium supplemented with 10% heat inactivated-foetal bovine serum (HI-FBS) and differentiated into macrophages with the addition of 20 ng/ml phorbol myristate acetate (PMA). For the intracellular killing experiment, macrophages (0.2 million/well/ml; 24 well plates) were infected with single-cell *M. tuberculosis* suspension at an MOI of 1:10. Following 4 h infection extracellular bacteria were removed by overlaying macrophages with RPMI containing 200 μg/ml of amikacin. Further, cells were washed twice with 1xPBS and infected macrophages were overlaid with RPMI containing drugs for 4 days. The infected macrophages were lysed on day 0 and day 4 post-exposure using 1x PBST (0.1% Triton X-100). For CFU enumeration 10.0 fold serial dilutions was prepared and 100 μl was plated on MB7H11 agar plates at 37 °C for 3−4 weeks.

4.5. Computational molecular docking studies

4.5.1. Protein structure preparations

The KatG crystal 1SJ2and 3WXO was obtained from Protein Data Bank (www.pdb.org) [35,36]. The crystal is found to be bounded with heme and glucose. The protein structure was optimized and subsequently minimized using Protein Preparation Wizard module of Maestro in which OPLS3 force field was used [38]. An additional crystal PDB ID: 3WXO, which is heme and INH bound was taken to observe the structural changes with different substrates.

4.5.2. Compounds preparation

The molecules **4a**, and **4b** were prepared using Schrödinger's module LIGPREP (version 2017−2), which generates tautomer's, and possible ionization states at the pH range 7 ± 2 using Epikand, also generates all the stereoisomers of the compound if necessary. The optimization was done using the OPLS3 force field [38].

4.5.3. Binding site identification

The most likely binding site of the compounds **4a**, and **4b** was identified using ligand independent (sitemap) and ligand dependent (molecular docking) methods.

4.5.4. SitMap analysis

Site-Map program of Schrodinger Suite was used for calculating binding site of **4a**, and **4b** [38,39]. The different parameters such as: site score, size, exposure score, enclosure, hydrophobic/hydrophilic character, contact, and donor/acceptor character were used for calculation of potential binding site [39,40]. Drugability of the site is denoted by D-score. The OPLS-2003 force field was employed, and a standard grid was used with 15 site points per reported site and cropped at 4.0 Å from the nearest site point.

4.5.5. Molecular docking

Molecular docking was used to assess the robustness of results provided by Sitemap. The docking studies were performed using AUTODOCK 4.2 [40]. The tools was required to identify the putative binding site as no co-crystal (with inhibitor) is reported for *M. tuberculosis*-katG, indeed, the INH bounded crystal is reported recently, which have shown more than one binding site [36]. The docking with AUTODOCK was performed using two different protocols: 1) Blind docking to explore the possible binding sites at the surface of KatG to rule out any biasedness, 2) Focused docking was performed on the most populated cluster obtained from blind docking by entering the docking grid on the center of mass of cluster representative conformation of INH. Two different approaches were performed as the most likely site identified by sitemap followed by the most populated cluster obtained through blind docking [40,41]. In all docking protocols, 200 conformers were generated separately to observe their convergence at the catalytic site. The grid coordinates, energy evaluations and generations of all three protocols were performed as previously described [40,41].

4.5.6. Energetic analysis

Free energy was carried out using the MMGBSA python script of AMBER tools and AMBER16 [41]. For this, the frames were extracted from the most stable state from the 300ns trajectory which was performed using the visual molecular dynamics tool (VMD). So, overall 1000 frames from all the complexes (COM1 and COM2) were subjected to energy calculations. The binding free energy (ΔG_{bind}) on each system was evaluated as follows:

$$\Delta G_{bind} = G_{com} - (G_{rec} + G_{lig}) \quad (1)$$

where G_{com}, G_{rec} and G_{lig} are the absolute free energies of complex, receptor and compounds, respectively, arranged over the equilibrium trajectory. According to free energy calculating method (MM/PBSA), the free energy difference can be decomposed as $\Delta G = \Delta E_{MM} + \Delta G_{solv} - T\Delta S_{conf}$, where$\Delta E_{MM}$ is the difference in molecular mechanics energy, ΔGs_{olv} the solvation energy (including an entropic contribution), and $T\Delta S_{conf}$ the solute configurational entropy (including the loss of translational and rotational entropy due to binding, as well as change in the vibrational entropy). The first two terms are calculated with the following equations:

$$\Delta E_{MM} = \Delta E_{bond} + \Delta E_{angle} + \Delta E_{torsion} + \Delta E_{vdw} + \Delta E_{elect} \quad (2)$$

$$\Delta G_{solv} = \Delta G_{PB} + \Delta G_{SA} \quad (3)$$

where E_{MM} includes the molecular mechanics energy contributed by bonded (E_{bond}, E_{angle}, and $E_{torsion}$) and nonbonded (E_{vdw} and E_{elect}) terms of the force field and ΔGsolv is the solvation free energy, which has an electrostatic (ΔG_{PB}, evaluated using the Poisson–Boltzmann equation) and a nonpolar contribution ($\Delta G_{SA} = \gamma\Delta SA + \beta$) proportional to the surface area (ΔSA).

Author's contribution

DM and RS conceived the idea, supervised the project and analysed the results. PS and RPS performed microbiology experiments. CLM, VK and AK contributed towards the synthesis of molecules. SA and AKT performed the computational studies.

Declaration of competing interest

The authors declare that they have no known competing financial interests or personal relationships that could have appeared to influence the work reported in this paper.

Acknowledgements

We would like to thank the Translational Health Science and Technology Institute (THSTI) for intramural research funding. PS acknowledges Department of Science and Technology for his fellowship (PDF/2018/002454). RS acknowledges the funding received from Department of Biotechnology (BT/PR29075/BRB/10/1699/2018).The authors are also thankful to Dr. David Alland and Dr. Pradeep Kumar for sharing Pks13 overexpression constructs. Dr. Bill Jacobs is also acknowledged for sharing INH resistant *M. tuberculosis* strain.

Appendix A. Supplementary data

Supplementary data to this article can be found online at https://doi.org/10.1016/j.ejmech.2020.112772.

References

[1] P. Glaziou, K. Floyd, M.C. Raviglione, Global epidemiology of tuberculosis, Epub 2018/08/03, Semin. Respir. Crit. Care Med. 39 (3) (2018) 271–285, https://doi.org/10.1055/s-0038-1651492. PubMed PMID: 30071543.

[2] S. Chakraborty, K.Y. Rhee, Tuberculosis drug development: history and evolution of the mechanism-based paradigm, Epub 2015/04/17, Cold Spring Harb Perspect Med 5 (8) (2015) a021147, https://doi.org/10.1101/cshperspect.a021147. PubMed PMID: 25877396; PubMed Central PMCID: PMCPMC4526730.

[3] C.K. Stover, P. Warrener, D.R. VanDevanter, D.R. Sherman, T.M. Arain, M.H. Langhorne, et al., A small-molecule nitroimidazopyran drug candidate for the treatment of tuberculosis, Epub 2000/07/06, Nature 405 (6789) (2000) 962–966, https://doi.org/10.1038/35016103. PubMed PMID: 10879539.

[4] R. Singh, U. Manjunatha, H.I. Boshoff, Y.H. Ha, P. Niyomrattanakit, R. Ledwidge, et al., PA-824 kills nonreplicating Mycobacterium tuberculosis by intracellular NO release, Epub 2008/11/29, Science 322 (5906) (2008) 1392–1395, https://doi.org/10.1126/science.1164571. PubMed PMID: 19039139; PubMed Central PMCID: PMCPMC2723733.

[5] Y. Li, F. Sun, W. Zhang, Bedaquiline and delamanid in the treatment of multidrug-resistant tuberculosis: promising but challenging, Epub 2018/12/15, Drug Dev. Res. 80 (1) (2019) 98–105, https://doi.org/10.1002/ddr.21498. PubMed PMID: 30548290; PubMed Central PMCID: PMCPMC6590425.

[6] A.H. Diacon, A. Pym, M.P. Grobusch, J.M. de los Rios, E. Gotuzzo, I. Vasilyeva, et al., Multidrug-resistant tuberculosis and culture conversion with bedaquiline, Epub 2014/08/21, N. Engl. J. Med. 371 (8) (2014) 723–732, https://doi.org/10.1056/NEJMoa1313865. PubMed PMID: 25140958.

[7] H. Li, D.H. Salinger, D. Everitt, M. Li, A. Del Parigi, C. Mendel, et al., Long-term effects on QT prolongation of pretomanid, alone and in combinations, in patients with tuberculosis, Epub 2019/07/31, Antimicrob. Agents Chemother. (2019), https://doi.org/10.1128/AAC.00445-19. PubMed PMID: 31358590.

[8] A. Bahuguna, D.S. Rawat, An overview of new antitubercular drugs, drug candidates, and their targets, Epub 2019/06/30, Med. Res. Rev. 40 (1) (2020) 263–292, https://doi.org/10.1002/med.21602. PubMed PMID: 31254295.

[9] I.D. Olaru, F. von Groote-Bidlingmaier, J. Heyckendorf, W.W. Yew, C. Lange, K.C. Chang, Novel drugs against tuberculosis: a clinician's perspective, Epub 2014/11/29, Eur. Respir. J. 45 (4) (2015) 1119–1131, https://doi.org/10.1183/09031936.00162314. PubMed PMID: 25431273.

[10] R. Dhiman, R. Singh, Recent advances for identification of new scaffolds and drug targets for Mycobacterium tuberculosis, Epub 2018/05/16, IUBMB Life 70 (9) (2018) 905–916, https://doi.org/10.1002/iub.1863. PubMed PMID: 29761628.

[11] R.S. Wallis, M. Maeurer, P. Mwaba, J. Chakaya, R. Rustomjee, G.B. Migliori, et al., Tuberculosis–advances in development of new drugs, treatment regimens, host-directed therapies, and biomarkers, Epub 2016/04/03, Lancet Infect. Dis.

16 (4) (2016) e34–e46, https://doi.org/10.1016/S1473-3099(16)00070-0. PubMed PMID: 27036358.
[12] D.T. Hoagland, J. Liu, R.B. Lee, R.E. Lee, New agents for the treatment of drug-resistant Mycobacterium tuberculosis, Epub 2016/05/08, Adv. Drug Deliv. Rev. 102 (2016) 55–72, https://doi.org/10.1016/j.addr.2016.04.026. PubMed PMID: 27151308; PubMed Central PMCID: PMCPMC4903924.
[13] T. Yuan, N.S. Sampson, Hit generation in TB drug discovery: from genome to granuloma, Epub 2018/02/01, Chem. Rev. 118 (4) (2018) 1887–1916, https://doi.org/10.1021/acs.chemrev.7b00602. PubMed PMID: 29384369; PubMed Central PMCID: PMCPMC5832989.
[14] F. Zani, P. Vicini, M. Incerti, Synthesis and antimicrobial properties of 2-(benzylidene-amino)-benzo[d]isothiazol-3-ones, Epub 2004/02/28, Eur. J. Med. Chem. 39 (2) (2004) 135–140, https://doi.org/10.1016/j.ejmech.2003.11.004. PubMed PMID: 14987822.
[15] I.M. Fakhr, M.A. Radwan, S. el-Batran, O.M. Abd el-Salam, S.M. el-Shenawy, Synthesis and pharmacological evaluation of 2-substituted benzo[b]thiophenes as anti-inflammatory and analgesic agents, Epub 2008/04/25, Eur. J. Med. Chem. 44 (4) (2009) 1718–1725, https://doi.org/10.1016/j.ejmech.2008.02.034. PubMed PMID: 18433939.
[16] R.J. Mourey, B.L. Burnette, S.J. Brustkern, J.S. Daniels, J.L. Hirsch, W.F. Hood, et al., A benzothiophene inhibitor of mitogen-activated protein kinase-activated protein kinase 2 inhibits tumor necrosis factor alpha production and has oral anti-inflammatory efficacy in acute and chronic models of inflammation, Epub 2010/03/20, J. Pharmacol. Exp. Therapeut. 333 (3) (2010) 797–807, https://doi.org/10.1124/jpet.110.166173. PubMed PMID: 20237073.
[17] W. Shi, T.L. Lowary, Structure-activity relationships in glycosylated 2-phenyl-indoles, 2-phenyl-benzo[b]thiophenes and 2-phenyl-benzo[b]furans as DNA binding and potential antitumor agents, Epub 2011/02/08, Bioorg. Med. Chem. 19 (5) (2011) 1779–1789, https://doi.org/10.1016/j.bmc.2011.01.014. PubMed PMID: 21296580.
[18] R. Wilson, P. Kumar, V. Parashar, C. Vilcheze, R. Veyron-Churlet, J.S. Freundlich, et al., Antituberculosis thiophenes define a requirement for Pks13 in mycolic acid biosynthesis, Epub 2013/06/19, Nat. Chem. Biol. 9 (8) (2013) 499–506, https://doi.org/10.1038/nchembio.1277. PubMed PMID: 23770708; PubMed Central PMCID: PMCPMC3720791.
[19] P. Singh, S.K. Kumar, V.K. Maurya, B.K. Mehta, H. Ahmad, A.K. Dwivedi, et al., S-enantiomer of the antitubercular compound S006-830 complements activity of frontline TB drugs and targets biogenesis of Mycobacterium tuberculosis cell envelope, Epub 2018/07/20, ACS Omega 2 (11) (2017) 8453–8465, https://doi.org/10.1021/acsomega.7b01281. PubMed PMID: 30023583; PubMed Central PMCID: PMCPMC6045410.
[20] C. Scheich, V. Puetter, M. Schade, Novel small molecule inhibitors of MDR Mycobacterium tuberculosis by NMR fragment screening of antigen 85C, Epub 2010/11/16, J. Med. Chem. 53 (23) (2010) 8362–8367, https://doi.org/10.1021/jm100993z. PubMed PMID: 21073150.
[21] D.A. Ibrahim, J. Boucau, D.H. Lajiness, S.K. Veleti, K.R. Trabbic, S.S. Adams, et al., Design, synthesis, and X-ray analysis of a glycoconjugate bound to Mycobacterium tuberculosis antigen 85C, Epub 2012/11/30, Bioconjugate Chem. 23 (12) (2012) 2403–2416, https://doi.org/10.1021/bc3004342. PubMed PMID: 23190459; PubMed Central PMCID: PMCPMC3548330.
[22] C. Grundner, D. Perrin, R. Hooft van Huijsduijnen, D. Swinnen, J. Gonzalez, C.L. Gee, et al., Structural basis for selective inhibition of Mycobacterium tuberculosis protein tyrosine phosphatase PtpB, Epub 2007/04/18, Structure 15 (4) (2007) 499–509, https://doi.org/10.1016/j.str.2007.03.003. PubMed PMID: 17437721; PubMed Central PMCID: PMCPMC2775457.
[23] A. Aggarwal, M.K. Parai, N. Shetty, D. Wallis, L. Woolhiser, C. Hastings, et al., Development of a novel lead that targets M. tuberculosis polyketide synthase 13, e25. Epub 2017/07/04, Cell 170 (2) (2017) 249–259, https://doi.org/10.1016/j.cell.2017.06.025. PubMed PMID: 28669536; PubMed Central PMCID: PMCPMC5509550.
[24] V.N. Khachatryan Dso, R.A. Sandu, V.N. Danilenko, A.V. Kolotaev, O.A. Zhdanovich, O.B. Bekker, K.R. Matevosyan, Quaternary Ammonium Derivatives of 2-Aminothiophen-3-Carboxylates Having Anti-tuberculosis Activity, 2017. RU 2629369 C1 20170829.
[25] G. Nikolakopoulos, H. Figler, J. Linden, P.J. Scammells, 2-Aminothiophene-3-carboxylates and carboxamides as adenosine A1 receptor allosteric enhancers, Epub 2005/11/30, Bioorg. Med. Chem. 14 (7) (2006) 2358–2365, https://doi.org/10.1016/j.bmc.2005.11.018. PubMed PMID: 16314104.
[26] S. Purser, P.R. Moore, S. Swallow, V. Gouverneur, Fluorine in medicinal chemistry, Epub 2008/01/17, Chem. Soc. Rev. 37 (2) (2008) 320–330, https://doi.org/10.1039/b610213c. PubMed PMID: 18197348.
[27] F.C. Odds, Synergy, antagonism, and what the chequerboard puts between them, Epub 2003/06/14, J. Antimicrob. Chemother. 52 (1) (2003) 1, https://doi.org/10.1093/jac/dkg301. PubMed PMID: 12805255.
[28] G. Arora, Behura A. Gagandeep, T.P. Gosain, R.P. Shaliwal, S. Kidwai, et al., NSC 18725, a pyrazole derivative inhibits growth of intracellular Mycobacterium tuberculosis by induction of autophagy, Epub 2020/02/18, Front. Microbiol. 10 (2019) 3051, https://doi.org/10.3389/fmicb.2019.03051. PubMed PMID: 32063889; PubMed Central PMCID: PMCPMC6999026.
[29] B. Lechartier, R.C. Hartkoorn, S.T. Cole, In vitro combination studies of benzothiazinone lead compound BTZ043 against Mycobacterium tuberculosis, Epub 2012/08/29, Antimicrob. Agents Chemother. 56 (11) (2012) 5790–5793, https://doi.org/10.1128/AAC.01476-12. PubMed PMID: 22926573; PubMed Central PMCID: PMCPMC3486603.
[30] V.M. Reddy, L. Einck, K. Andries, C.A. Nacy, In vitro interactions between new antitubercular drug candidates SQ109 and TMC207, Epub 2010/04/14, Antimicrob. Agents Chemother. 54 (7) (2010) 2840–2846, https://doi.org/10.1128/AAC.01601-09. PubMed PMID: 20385864; PubMed Central PMCID: PMCPMC2897281.
[31] C. Vilcheze, W.R. Jacobs Jr., Resistance to isoniazid and ethionamide in Mycobacterium tuberculosis: genes, mutations, and causalities, MGM2-0014-2013. Epub 2015/06/25, Microbiol. Spectr. 2 (4) (2014), https://doi.org/10.1128/microbiolspec.MGM2-0014-2013. PubMed PMID: 26104204; PubMed Central PMCID: PMCPMC6636829.
[32] W. Shi, X. Zhang, X. Jiang, H. Yuan, J.S. Lee, C.E. Barry 3rd, et al., Pyrazinamide inhibits trans-translation in, Epub 2011/08/13, Mycobacterium Tuberculosis. Sci. 333 (6049) (2011) 1630–1632, https://doi.org/10.1126/science.1208813. PubMed PMID: 21835980; PubMed Central PMCID: PMCPMC3502614.
[33] N.E. Caceres, N.B. Harris, J.F. Wellehan, Z. Feng, V. Kapur, R.G. Barletta, Overexpression of the D-alanine racemase gene confers resistance to D-cycloserine in Mycobacterium smegmatis, Epub 1997/08/01, J. Bacteriol. 179 (16) (1997) 5046–5055, https://doi.org/10.1128/jb.179.16.5046-5055.1997. PubMed PMID: 9260945; PubMed Central PMCID: PMCPMC179361.
[34] J. Suarez, K. Ranguelova, A.A. Jarzecki, J. Manzerova, V. Krymov, X. Zhao, et al., An oxyferrous heme/protein-based radical intermediate is catalytically competent in the catalase reaction of Mycobacterium tuberculosis catalase-peroxidase (KatG), Epub 2009/01/14, J. Biol. Chem. 284 (11) (2009) 7017–7029, https://doi.org/10.1074/jbc.M808106200. PubMed PMID: 19139099; PubMed Central PMCID: PMCPMC2652337.
[35] T. Bertrand, N.A. Eady, J.N. Jones, Jesmin, J.M. Nagy, B. Jamart-Gregoire, et al., Crystal structure of Mycobacterium tuberculosis catalase-peroxidase, Epub 2004/07/03, J. Biol. Chem. 279 (37) (2004) 38991–38999, https://doi.org/10.1074/jbc.M402382200. PubMed PMID: 15231843.
[36] S. Kamachi, K. Hirabayashi, M. Tamoi, S. Shigeoka, T. Tada, K. Wada, The crystal structure of isoniazid-bound KatG catalase-peroxidase from Synechococcus elongatus PCC7942, Epub 2014/10/11, FEBS J. 282 (1) (2015) 54–64, https://doi.org/10.1111/febs.13102. PubMed PMID: 25303560.
[37] S. Kidwai, R. Bouzeyen, S. Chakraborti, N. Khare, S. Das, T. Priya Gosain, et al., NU-6027 inhibits growth of Mycobacterium tuberculosis by targeting protein kinase D and protein kinase G, Epub 2019/07/10, Antimicrob. Agents Chemother. 63 (9) (2019), https://doi.org/10.1128/AAC.00996-19. PubMed PMID: 31285226; PubMed Central PMCID: PMCPMC6709498.
[38] S. Asthana, S. Shukla, A.V. Vargiu, M. Ceccarelli, P. Ruggerone, G. Paglietti, et al., Different molecular mechanisms of inhibition of bovine viral diarrhea virus and hepatitis C virus RNA-dependent RNA polymerases by a novel benzimidazole, Epub 2013/05/01, Biochemistry 52 (21) (2013) 3752–3764, https://doi.org/10.1021/bi400107h. PubMed PMID: 23627712.
[39] S. Kant, S. Asthana, D. Missiakas, V. Pancholi, A novel STK1-targeted small-molecule as an "antibiotic resistance breaker" against multidrug-resistant Staphylococcus aureus, Epub 2017/07/13, Sci. Rep. 7 (1) (2017) 5067, https://doi.org/10.1038/s41598-017-05314-z. PubMed PMID: 28698584; PubMed Central PMCID: PMCPMC5505960.
[40] S. Asthana, P. Zucca, A.V. Vargiu, E. Sanjust, P. Ruggerone, A. Rescigno, Structure-activity relationship study of hydroxycoumarins and mushroom tyrosinase, Epub 2015/08/12, J. Agric. Food Chem. 63 (32) (2015) 7236–7244, https://doi.org/10.1021/acs.jafc.5b02636. PubMed PMID: 26263396.
[41] M. Srivastava, C. Suri, M. Singh, R. Mathur, S. Asthana, Molecular dynamics simulation reveals the possible druggable hot-spots of USP7, Epub 2018/10/23, Oncotarget 9 (76) (2018) 34289–34305, https://doi.org/10.18632/oncotarget.26136. PubMed PMID: 30344943; PubMed Central PMCID: PMCPMC6188144.